LOW p_T PHYSICS AT THE $\bar{p}$-p COLLIDER*

By A. Capella

Laboratoire de Physique Théorique et Hautes Energies, Université de Paris-Sud, 91405 Orsay, France

(Received April 12, 1984)

The low p_T results at the SPS colliders are compared with the expectations from conventional theories (Regge-Muller, string models, parton model for sort processes, etc.). Most of the short range order properties of the produced particles, predicted in these theories are badly violated but a few of them are satisfied to a good accuracy. We show that the multi-chain dual parton model allows us to describe the whole picture.

PACS numbers: 13.85.-t

1. Introduction

The conventional theories of low p_T hadronic interactions (Regge-Muller, Feynman's parton approach, string models, etc.) are characterized at the production level, by the so-called short-range order (SRO) property. SRO means that the dynamical correlations between produced particles have short-range in rapidity.

Some important consequences of the SRO picture are listed below: (1) the density of particles in the central region dN/dy is independent of y (rapidity plateau); (2) the plateau height is independent of s; (3) the extension of the plateau increases as $\log s$; (4) in the fragmentation regions dN/dy is independent of s at fixed $y-y_{max}$, i.e. at fixed distance from the edges of phase space; (5) the average multiplicity $\langle N\rangle$ increases like $\log s$; (6) the ratio $D/\langle N\rangle$, where $D=[\langle N^2\rangle-\langle N\rangle^2]^{1/2}$, and all the moments $C_k=\langle N^k\rangle/\langle N\rangle^k$ of the multiplicity distribution decrease when s increases; (7) there are no dynamical long-range correlations (LRC). Correlations between particles produced at rapidities y_1 and y_2 with $|y_1-y_2|>\lambda$ (where λ is some correlation length, typically $\lambda\sim 1.5$–2 units) should go to zero as s increases; (8) Quantum numbers (like electric charge) are locally conserved; (9) the average p_T is independent of s; (10) the average p_T is independent of the event multiplicity; (11) the elastic amplitude obtained via unitarity has a slope which increases as $\log s$ (shrinking of the diffraction plateau).

How this scenario compare with $\bar{p}p$ collider data? It turns out that all these predic-

* Presented at the XXII Cracow School of Theoretical Physics, Zakopane, Poland, May 30 — June 9, 1982.

tions are rather badly violated, except for (4), (8), (10) and (11), where the situation is as follows: (4) the presently available data do not extent to large values of x. However, the scaling property (4) seems to be verified [1] (at least at a $15 \div 20\%$ level, whereas the property (2) is violated by more than 100% between ISR and collider energies; (8) local compensation of charge has not been tested at collider energies. However, it is very well verified at lower energies; (10) $\langle p_T \rangle$ increases rather mildly (from about 0.35 to 0.42 GeV)

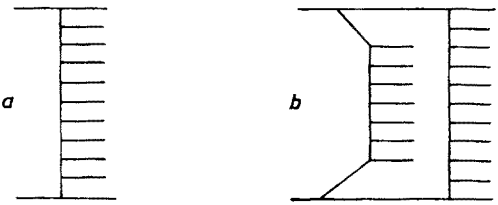

Fig. 1a. Single inelastic scattering. b. Double inelastic scattering. Note that multiple inelastic collisions involve different constituents of the colliding hadrons

from ISR to collider energies and part of this rise is due to the flattering of the large p_T tail; (11) the elastic peak continues to shrink but the slope near $t = 0$ increases faster than $\log s$.

In view of this, must we conclude that the conventional approach fails? The answer is clear if one takes the conventional approach literally. However, the Regge-Muller approach for instance is a fairly general one. It is formulated in the framework of an S-matrix theory and unitarity is known to play a very important role. One knows that inelastic rescattering (Fig. 1) introduces long-range dynamical correlations — and thus violates SRO [2]. The physical origin of these LRC is the following: if one observes a large multiplicity fluctuation in a given rapidity interval, one is most probably observing a contribution corresponding to several inelastic rescatterings (due to SRO in each inelastic collision, it is very unprobable that such a large multiplicity fluctuations occurs in a single inelastic collision). Thus, one is bound to observe large multiplicity fluctuations far away in rapidity; hence a positive LRC.

In what follows we are going to show that the presence of these inelastic rescattering terms, with weights given by standard unitarization schemes (eikonal or perturbative reggeon calculus) allows one to understand the features of the data described above, assuming that SRO is verified within each individual inelastic collision. This is true provided that the particles produced in inelastic rescattering have a well-defined rapidity structure. This structure is precisely the one obtained in the framework of the multi-chain dual parton model [3].

2. *The dual parton model [8, 10, 18]*

The aim of this model is to find the mechanism responsible for multi-hadron production in low p_T hadronic interactions. This can be obtained from very general topological arguments known as the $1/N$ expansion. These arguments were introduced by t'Hooft [4] for

non-perturbative QCD and extended by Veneziano [5] in such a way that unitarity is enforced.

The physical idea at the basis of the $1/N$ expansion is very simple: since one cannot use a power expansion in terms of the (large) coupling constant, one has to find a different type of expansion. It turns out that the topological properties of a diagram provide a basis for such an expansion; the diagram with the simplest topology dominates; by complicat-

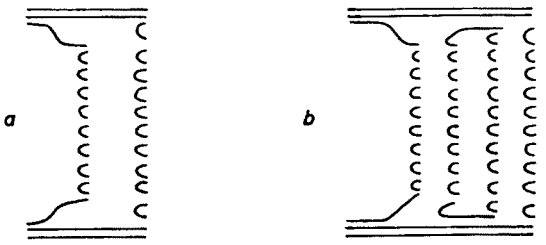

Fig. 2a. Single inelastic scattering in a $\bar{p}p$ interaction in the dual parton model. Hadrons are produced in two chains $q\bar{q}$–qq and $\bar{q}_v$–q_v. b. Example of double inelastic collision in the dual parton model. The extra chains of hadrons are produced linking sea quarks and antiquarks from the colliding hadrons

ing the topology of a graph its contribution to the total cross-section goes down by powers of $(1/N)^2$, where N is the number of colors or flavors.

The mechanism of multi-hadron production which emerges from these topological arguments is the following. Let us consider the case of a $\bar{p}p$ collision. As a result of the interaction (a complicated gluon exchange mechanism) the proton splits into a valence quark and an antiquark and the $\bar{p}$ into $\bar{q}_v$ and $q\bar{q}$. Two chains of hadrons are produced: one chain is stretched between q_v and $\bar{q}_v$ and the second one between qq and $q\bar{q}$ (see Fig. 2a). This is the dominant term in the $1/N$ expansion which survives as $s \to \infty$ and corresponds to one single inelastic collision. The next term is shown in Fig. 2b. Here four chains of hadrons are produced: the two former chains plus two new chains which are stretched between sea constituents of the colliding hadrons (sea quarks and antiquarks in the example shown in Fig. 2b). This term corresponds to a double inelastic collision[1]. More generally, a term corresponding to k inelastic collisions will contain $2k$ chains. In order to compute the contributions of the various terms to the physical quantities relative to multi-hadron production, one needs three ingredients: 1) the momentum distribution function of the constituents in the hadron, 2) the fragmentation function of these (colored) constituents, 3) the relative weights (cross-sections) of the various terms in the $1/N$ expansion.

The momentum distribution functions can be obtained from the general features of the model. One uses only soft physics arguments. The behaviour near $x = 0$ of the mo-

[1] It is easy to understand that such a term gives a smaller contribution to σ_T than the previous one (Fig. 2a). Indeed it involves a fluctuation in the proton wave function consisting of the three valence quarks plus a $q\bar{q}$ pair from the sea. One has of course to link the four constituents of each colliding hadrons in all possible ways (for instance qq–q_s, $q\bar{q}$–$\bar{q}_s$, q_v–$\bar{q}_s$ and $\bar{q}_v$–q_s). All these possibilities lead however, to very similar results. For all physical quantities discussed in the text, the results obtained with different ways of linking the constituents differ from one another by less than 5 per cent

mentum distribution of the various constituents is identical to the corresponding behaviour of parton structure functions. The valence quarks are slow in average (with a $1/\sqrt{x}$ behaviour near $x = 0$) and the sea quarks and antiquarks are even slower (in $1/x$). Since these are constituents, the sum of their momentum fractions adds up to one. Therefore, the diquarks are fast in average. Since they carry the baryon quantum numbers one can understand in this way the leading particle effect. One obtains the following momentum distribution function for a proton or antiproton [3]

$$\varrho_k(x_1, x_2, \ldots x_{2k}) = C_k \frac{1}{\sqrt{x_1}} \frac{1}{x_2} \ldots x_{2k}^{1.5} \delta(1-x_1-x_2 \ldots -x_{2k}). \tag{1}$$

Here the index 1 refers to the valence quark, $2k$ refers to the diquark and the other indices refer to the sea constituents. C_k is chosen in such a way that ϱ_k is normalized to one. (The above equation has the structure of a Kuti-Weisskopf model, except that here it appears at an exclusive level.)

Let us turn now to the second point. Here the model does not provide an equally specific anwer so that the fragmentation function have to be introduced as an input external to the model. For the numerical calculations we use the standard parton model (scaling) quark and diquark fragmentation functions (universality ansatz). However, at a semi-quantitative level, all the results discussed below are independent of the exact form of the fragmentation functions.

Turning next to the weights of the various contributions, they cannot be computed due to the fact that the diagrams involved correspond in fact to an infinite sum of QCD diagrams with an arbitrary number of gluon and $q\bar{q}$ loops exchanged. However, as explained above, the various contributions in the $1/N$ expansion are in a one to one correspondence [5] with unitarity corrections as they appear in the perturbative reggeon calculus expansion. Practically, this means that all weights can be computed in terms of a few arbitrary parameters – which are determined from experimental data (σ_{tot}, σ_{el}, σ_{DD} etc.) [22]. Two complete fits of the data are available in the literature [6, 7]. We have used the weights obtained from both sets of parameters. The results are almost the same in the two cases. It is interesting to notice that the parameters obtained with data up to ISR energies, give a good description of σ_{T} at collider energies (Fig. 3). One also obtains a slope of the elastic peak at $t \simeq 0$ equal to 16 GeV^{-2}, which is consistent with the collider value and corresponds to a shrinking of the diffraction peak faster than $\log s$.

Using the three ingredients discussed above one obtains the following expression for the rapidity density (see previous footnote).

$$\frac{dN^{\bar{p}p}}{dy} \equiv \frac{1}{\sigma_{\text{in}}} \frac{d\sigma^{\bar{p}p}}{dy} \equiv N^{\bar{p}p}(y) = \frac{1}{\sigma_{\text{in}}} \sum_{k=1}^{\infty} \sigma_k$$

$$[N^{q\bar{q}-qq}(y) + N^{\bar{q}_v-q_v}(y) + (2k-2)N^{\bar{q}_s-q_s}(y)]$$

$$\approx N^{q\bar{q}-qq}(y) + N^{\bar{q}_v-q_v}(y) + (2\langle k\rangle - 2)N^{\bar{q}_s-q_s}(y), \tag{2}$$

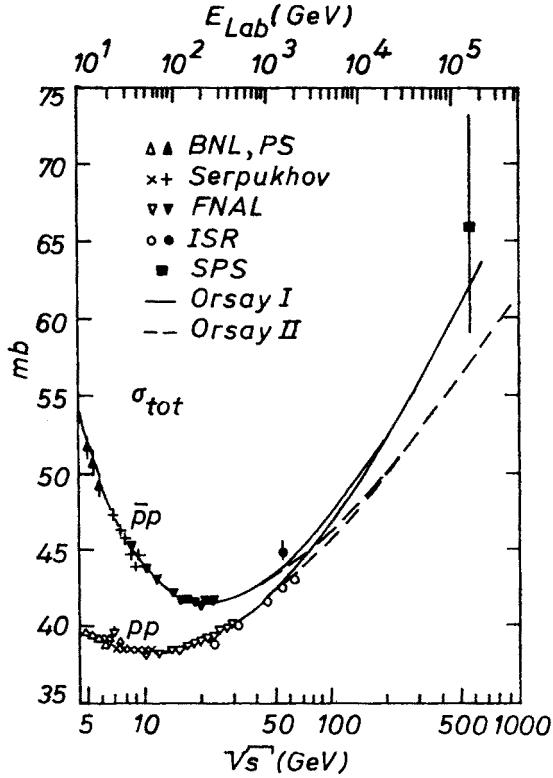

Fig. 3. Values of σ_{tot} for pp and $\bar{p}p$ up to $\sqrt{s} = 540$ GeV obtained from the Orsay (full line) and ITEP (dotted line) fits in the framework of the perturbative reggeon calculus. Only data up to ISR energies were available when these fits were done. The extrapolation to collider energy is quite reasonable

where

$$\sigma_{in} = \sum_{k=1}^{\infty} \sigma \quad \text{and} \quad \langle k \rangle = \sum_{k=1} k\sigma_k/\sigma_{in}.$$

With the weights obtained in the perturbative reggeon calculus $\langle k \rangle$ has a mild energy dependence. It grows from about 1.5 to about 2 from low ISR to collider energies.

$N^{\bar{q}q-qq}(y)$ etc., are the rapidity densities of the individual chains. They are obtained from a convolution of the momentum distribution and fragmentation functions, and therefore contain no free parameter. Since both momentum distribution and fragmentation functions scale, the height of each of the individual chains is the same at $s \to \infty$. However, as a result of the convolution (and due partly to the physical thresholds of the chains), one obtains a height which is bigger (smaller) for the longer (shorter) chains. The result of the convolution at $\sqrt{s} = 63$ GeV and 540 GeV is shown in Fig. 4 for the different ichans.

The main two features of the model which depend only on ingredient number 1 are a) the fact that a valence quark is slowed down (held back effect), b) the excess of particles

produced in a multiple inelastic collision (as compared to a single one) is concentrated in the central rapidity region. In other words the invariant mass of the q_s–$\bar{q}_s$ (rescattering) chains is much smaller than $\sqrt{s}$. Typically it has 3 to 5 GeV in average at ISR energies, and 50 GeV at collider energy.

Point a) has to be checked at ISR energies. Indeed, because the average position of the edges of the various chains is fixed in x, the difference between the rapidity values of the chain edges and the edge of phase space is independent of s. For the valence quark

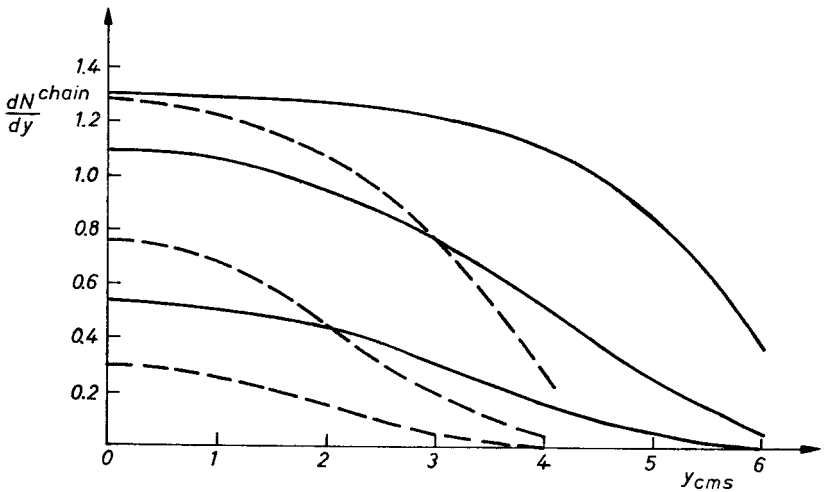

Fig. 4. The rapidity density of secondaries produced in the various chains at $\sqrt{s}$ = 540 GeV (full lines) and 63 GeV (dashed lines). The higher (lower) curves correspond to the $\bar{q}q$–qq ($\bar{q}_s$–q_s) chains — the intermediate one corresponding to the $\bar{q}_v$–q_v ones. These curves are obtained from a convolution of momentum distribution and fragmentation functions

this distance is typically 2 to 3 rapidity units. Thus at ISR energies the "held-back" valence quark is close enough to $y^* = 0$ to have an effect there, while at collider energies it has already moved into the fragmentation regions. On the contrary, point b) can only be checked at collider energies. Indeed, at ISR energies the q_s–$\bar{q}_s$ are very short and low in height and their contribution is essentially negligible.

A discussion concerning a possible test of point a) can be found in Ref. [8] and will not be repeated here since it concerns the ISR energy range.

Let me notice only that the held-back effect is also required in the framework of the dimensional counting rules [9]. Thus instead of using parton model fragmentation function for constituent quarks, one could use dimensional counting rules instead (which guarantees a reasonably good description of the fragmentation regions).

In what follows I am going to show that point b) is the key feature which allows one to understand the low p_T data at collider energy. I shall also argue that some of these data (namely the long-range forward backward correlation slopes) provide a crucial test of point b).

3. Results

In this Section I present the results of the model for the various quantities discussed in the Introduction. It should be noted that the model of Section 2 (including the rescattering chains) and some of the results below (including the prediction of a charged density of 3.5 at $y^* = 0$) were given in Ref. [10] before the colliders started to operate.

a) Plateau width and height [3]

The rapidity distributions at ISR and collider energies can be obtained immediately from Eq. (2) and Fig. 4. (Notice that the second expression in Eq. (2) involves an approximation and should only be applied in the central region.)

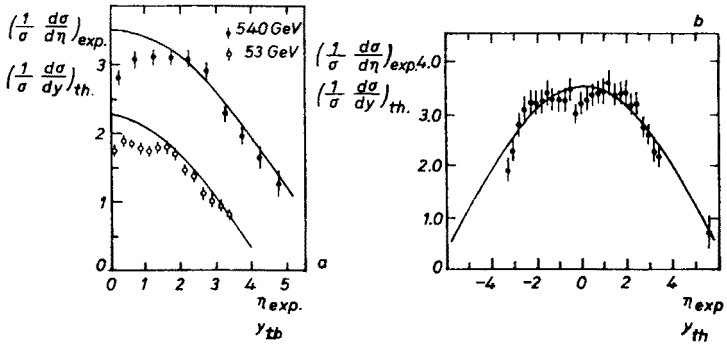

Fig. 5. The charged particle rapidity distribution at $\sqrt{s} = 540$ and $\sqrt{s} = 53$ GeV are compared with the UA5 (Fig. 5a) and UA1 (Fig. 5b) data

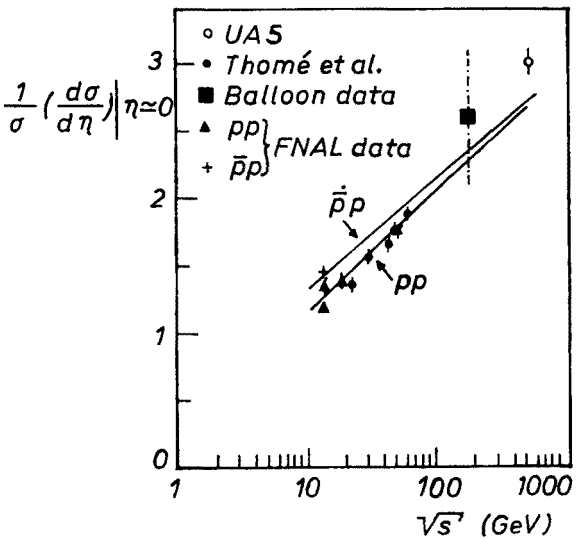

Fig. 6. The central plateau height $1/\sigma\ (d\sigma/dy)$ $(y^* = 0)$ compared with the data for $1/\sigma\ d\sigma/dy$ $(\eta^* = 0)$. The comparison is meaningful since the ratio of these two quantities is expected to be independent of s

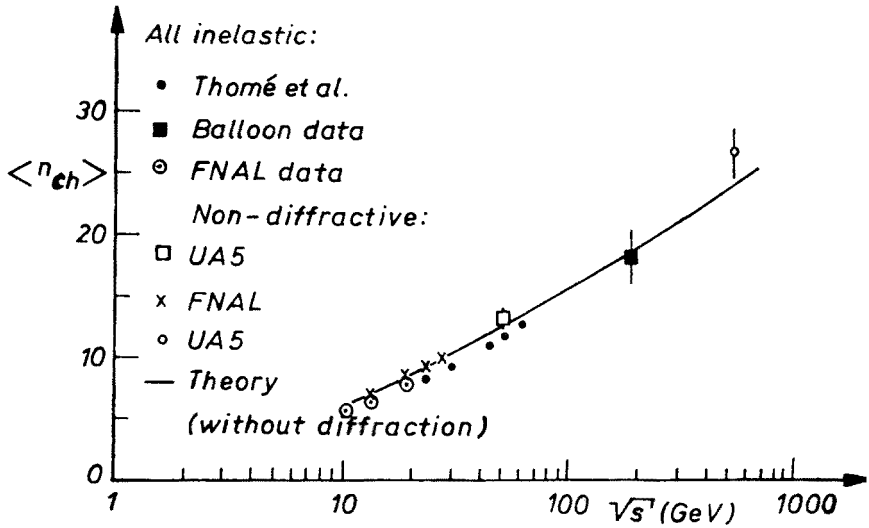

Fig. 7. The average pp charged multiplicity as a function of s. The theoretical value of the $\bar{p}p$ multiplicity at $\sqrt{s} = 540$ GeV is only 1% higher than the pp one

Some results are shown in Figs 5–7. It is clear from Fig. 4 that the increase of the plateau is mostly due to the increase of the height in the chains q_s–$\bar{q}_s$ (and also q_v–$\bar{q}_v$) with energy. Only a small fraction of the rise is due to the variation of $\langle k \rangle$ with s. Since the q–$\bar{q}$ chains have a small invariant mass, their rapidity distributions do not exhibit a plateau (as does the chain qq–$\bar{q}\bar{q}$ at $\sqrt{s} = 540$ GeV). With increasing energies the contribution of the q–$\bar{q}$ chains becomes more and more important and the plateau is practically destroyed – the center of the rapidity distribution being pushed upwards.

b) Rapidity distributions as a function of the multiplicity [3]

If one considers the rapidity distributions corresponding to events in multiplicity bands with increasing number of particles, the results of the model are also quite straightforward. As discussed above, by increasing the multiplicity one is considering contribu-

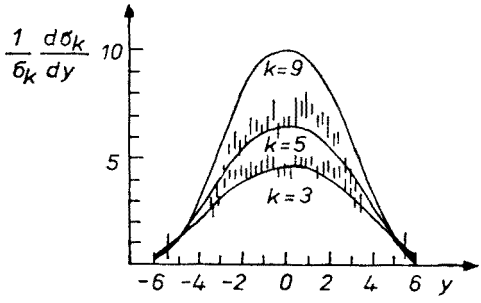

Fig. 8. Variation of the plateau height as a function of the charged multiplicity. The value of N_{ch} corresponding to a given k is obtained by integrating $(1/\sigma_k)d\sigma_k/dy$ over the rapidity. The ratio $(d\sigma/d\eta)/(d\sigma/dy) = 0.87$ at $y = 0$ has been assumed

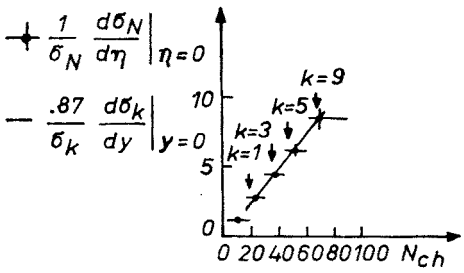

Fig. 9. $(1/\sigma_k)\, d\sigma_k/dy$ at three different values of k. The experimental points are the values of $1/\sigma_n\, d\sigma_n/d\eta$ in the two multiplicity bands (in the pseudorapidity range $|\eta| < 3.5$), $21 < N_{ch} < 30$ (lower data) and $31 < N_{ch} < 40$ (upper data). The central value of N_{ch} in these bands correspond roughly to $k = 3$ and 5, respectively

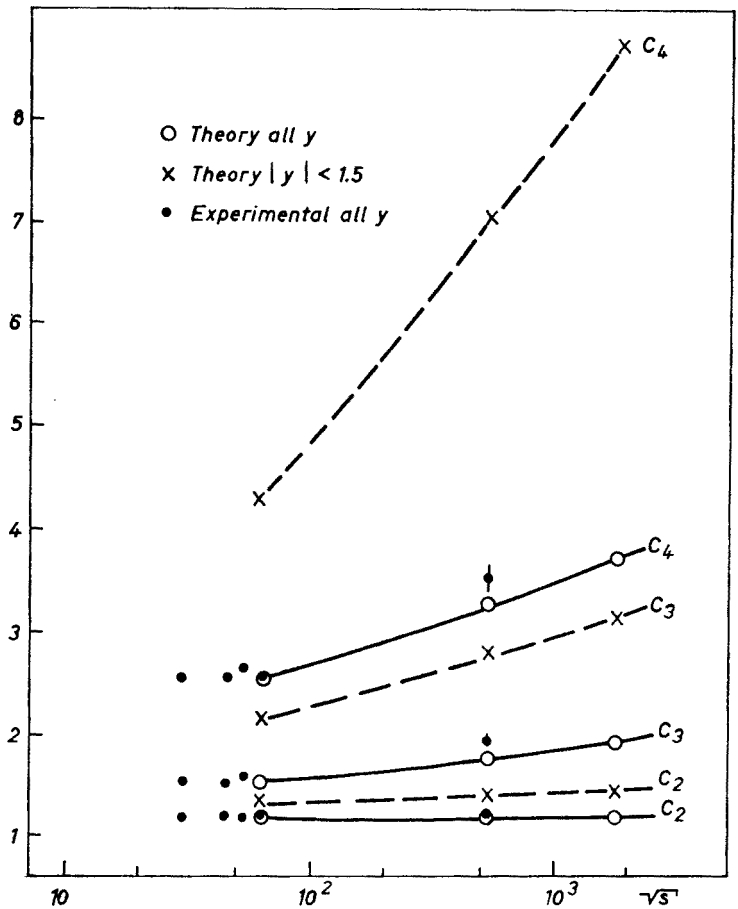

Fig. 10. The values of the multiplicity moments C_i are plotted as a function of the energy and compared with ISR [8] and UA5 [9] data. The full and dotted lines through the theoretical points are only to guide the eye

tions containing an increasing number of rescattering chains (q_s–$\bar{q}_s$). Thus the rapidity distributions will grow higher and narrower and they will cross-over at a value of y corresponding to the edge of these chains (which is roughly $|x| \sim 0.1$). This is shown in Fig. 8 and compared with data from the UA1 collaboration [11]. Also every time that an extra q_s–$\bar{q}_s$ chain is added one increases both the multiplicity and the "plateau" height in a well defined way. One obtains in this way a linear dependence of $(dN/dy)_{y=0}$ with multiplicity with a slope which agrees very well with the data from the UA5 collaboration [11] (see Fig. 9).

c) Scaling in the fragmentation regions [3]

Since the q_s–$\bar{q}_s$ chains are practically concentrated in the region $|x| \lesssim 0.1$ one expects that the rapidity distributions will be roughly independent of s in the region $|x| > 0.1$. Numerical calculations show that the scaling violation is at most 6% in the range $0.1 < x < 0.8$.

d) Multiplicity distributions [22]

In order to compute the various moments of the multiplicity distribution, we assume that the particles produced in two different chains are uncorrelated and that there are only short-range rapidity correlations within each chain. More precisely we assume independent emission of light clusters within each chain, each cluster decaying in average into K charged particles. (We use $K = 1.4$ corresponding to standard resonances.) The results for non-diffractive events at $\sqrt{s} = 63$, 540 and 1800 GeV are shown in Fig. 10 – both for the complete rapidity interval and for a central region of fixed length $|y| < 1.5$. In both cases the higher moments increase with s, indicating that the multiplicity distribution develops a high multiplicity tail of increasing height as s increases (and thus KNO scaling is violated). The moments and their s-dependence are larger in the central interval $|y| < 1.5$. The comparison with available data is shown in Table I.

e) Long-range rapidity correlations [22, 3]

The long-range forward-backward rapidity correlations provide a crucial test of point b) in Section 2. They are a unique measurement in which the contribution of the rescattering chains is isolated from that of the (dominant) single inelastic ones. One measures the average multiplicity in the backward hemisphere as a function of the event multiplicity in the forward one. This kind of plot is customary in probability theory where it is known as a linear regression plot. Under fairly general conditions, one obtains a linear relation

$$\langle N_B \rangle = a + bN_F,$$

where

$$a = \langle N_B \rangle - b\langle N_F \rangle$$

and

$$b = \frac{\langle N_F N_B \rangle - \langle N_F \rangle \langle N_B \rangle}{\langle N_F^2 \rangle - \langle N_F \rangle^2}.$$

TABLE I

Theoretical results for C_k and γ_k for non-diffractive events at $\sqrt{s} = 63$ and 540 GeV for both the whole rapidity interval and the central region $|y| < 1.5$. These values are taken from Tables I and VI of Ref. [22]. The experimental results at the colliders [24] and at ISR for all y [23] are also for non-diffractive events. The comparison with the theoretical predictions is very good in all these cases. The ISR data for $|y| < 1.5$ [25] contain single diffraction and thus the comparison with theory is not very meaningful. Note however, that the result of removing diffractive events is to decrease the values of γ_i. It is therefore clear that KNO scaling is also violated in the central region $|y| < 1.5$, contrary to the claim in Ref. [24]

	$\sqrt{s} = 63$ GeV (All y)		$\sqrt{s} = 540$ GeV (All y)	
	Theory	Exp.	Theory	Exp.
C_2	1.19	1.20 ± 0.01	1.25	1.31 ± 0.04
C_3	1.65	1.67 ± 0.03	1.94	2.12 ± 0.14
C_4	2.57	2.63 ± 0.09	3.66	4.05 ± 0.40
C_5	4.44	4.60 ± 0.2	8.10	8.8 ± 1.3
γ_2	0.19	0.20 ± 0.01	0.25	—
γ_3	0.07	0.06 ± 0.01	0.19	—
γ_4	0.04	—	0.21	—
	$\sqrt{s} = 63$ GeV ($\|y\| < 1.5$)		$\sqrt{s} = 540$ GeV ($\|y\| < 1.5$)	
	Theory	Exp. (Diffraction included)	Theory	Exp.
C_2	1.34	—	1.48	—
C_3	2.23	—	3.03	—
C_4	4.38	—	7.91	—
C_5	9.75	—	24.8	—
γ_2	0.34	0.46 ± 0.01	0.48	0.52 ± 0.01
γ_3	0.20	0.34 ± 0.02	0.58	0.53 ± 0.05
γ_4	0.17	0.29 ± 0.05	1.00	0.80 ± 0.18

A value $b \neq 0$ indicates a correlation between the F and B hemispheres. In order to check whether or not such a correlation has a long-range in rapidity, one makes an experimental cut which excludes the particles in the region $|y| \leqslant 1$. In this case, if the resulting value of the slope, b_{LR}, is different from zero, one is sure that the correlation has a long-range in rapidity.

In the dual parton model one can compute b_{LR} by assuming that the particles produced in the individual chains obey SRO and that two different chains are uncorrelated, i.e.,

$$\langle N^{\text{chain } i}(y), N^{\text{chain } i}(y') \rangle = \langle N^{\text{chain } i}(y) \rangle \langle N^{\text{chain } i}(y') \rangle \tag{3}$$

for $|y - y'| > 2$, and

$$\langle N^{\text{chain } i}(y), N^{\text{chain } i'}(y') \rangle = \langle N^{\text{chain } i}(y) \rangle \langle N^{\text{chain } i'}(y') \rangle. \tag{4}$$

TABLE II

The average charged multiplicity, the F–B long range correlation slope b and its numerator for non-diffractive events at ISR, SPS collider and Tevatron energies for different sizes and positions of the F and B rapidity intervals

$\sqrt{s}$	Rapidity interval	$\langle N_F \rangle$	$\langle N_F N_B \rangle - \langle N_F \rangle \langle N_B \rangle$	b^{theory}	$b^{\text{experiment}}$
63	$1 < \lvert y \rvert < 4$	3.94	0.43	0.06	0.156+0.013
540	$\lvert y \rvert > 1$	10.87	12.8	0.36	
540	$1 < \lvert y \rvert < 4$	8.47	12.5	0.43	0.41+0.01
540	$1 < \lvert y \rvert < 2$	3.38	2.98	0.37	0.36+0.02
540	$3 < \lvert y \rvert < 4$	2.21	0.38	0.06	0.04+0.02
1800	$\lvert y \rvert > 1$	14.87	30.93	0.49	
1800	$1 < \lvert y \rvert < 4$	9.95	23.88	0.53	

Squaring Eq. (2) and using the above relations one obtains

$$[\langle N_F N_B \rangle - \langle N_F \rangle \langle N_B \rangle]_{LR} \simeq 4[\langle K^2 \rangle - \langle K \rangle^2] \langle N_F^{q_s - \bar{q}_s} \rangle \langle N_B^{q_s - \bar{q}_s} \rangle. \tag{5}$$

Here the quantity in brackets is the square of the dispersion in the number of inelastic collisions and $\langle N_F^{q_s-\bar{q}_s} \rangle$ ($\langle N_B^{q_s-\bar{q}_s} \rangle$) is the multiplicity in one rescattering chain q_s–$\bar{q}_s$ in the forward (backward) rapidity interval one is considering. We see that a long-range correlation is introduced due to the fluctuation in the number of chains. In fact Eq. (5) is only an approximate expression for the numerator of b_{LR}. Strictly speaking Eqs (3) and (4) should be applied only for fixed positions of the ends of the chains and the fact that the position of the chain ends are distributed according to Eq. (1) introduces an extra contribution to the correlation – which decreases with increasing energy. All this has been taken into account in the numerical calculations. However, for the physical discussion we use Eq. (5) which is more transparent.

The crucial test of the dual parton model referred to above is obtained by studying the variation of b_{LR} as a function of the gap size. More precisely let us consider the long-range correlation between particles produced in the two rapidity intervals $y_0 \leqslant y \leqslant y_0 + 1$ and $-y_0 - 1 \leqslant y' \leqslant -y_0$. In view of the small rapidity length of the q_s–$\bar{q}_s$ chains, Eq. (5) leads to a strong decrease of b_{LR} with increasing values of y_0. This result is a characteristic feature of the dual parton model which predicts a very dramatic decrease of b_{LR} when y_0 increases from 1 to 3, and has been measured by the UA5 collaboration [14, 15]. In Table II the results of the model are given and compared with available data.

f) Local compensation of quantum numbers [2]

Multiple-scattering models have the peculiar feature on introducing long-range correlations without violating the local compensation of charge typical of the models with SRO. More precisely the second-order zone correlation function (the only measured until now) is not affected by multiple-scattering terms, whereas the fourth-order and higher order correlation functions are affected in a specific way.

In order to study the local compensation of charge, one introduces a random function $Z(y)$ representing the transfer of the electric charge across the rapidity value y. The charge is locally compensated when the moment functions $\langle Z(y_1) \ldots Z(y_k)\rangle$ exhibit short-range order properties. For instance $\langle Z(y)Z(y')\rangle$ has to decrease rapidly towards zero with increasing $|y-y'|$. Notice that, for symmetry reasons, the moment functions of odd order must vanish — provided all the rapidities are far from the kinematical boundaries. It follows immediately from this last property and Eq. (5) that no long-range correlations are introduced at the level of the two-point functions. Well defined violations of the local compensation of charge are introduced at the level of the four-point function. Unfortunately an experimental study of this function requires enormous statistics and is therefore very difficult.

g) Correlation between $\langle p_T\rangle$ and multiplicity [16]

An interesting correlation has been observed [17] between $\langle p_T\rangle$ and multiplicity at the collider. In the rapidity window $|y| < 2.5$, $\langle p_T\rangle$ increases from 0.33 to 0.47 GeV/c when the multiplicity per unit rapidity increases from 1 to 20. A possible explanation of this correlation in the framework of the multiple-scattering models is the following. Due to the intrinsic transverse momentum, $\vec{K}_T$, of the constituents at the ends of the chains, the chains are "tilted", i.e. the CMS of the chain does not coincide with the CMS of the reaction. One has

$$\vec{p}_T = \vec{p}_{T'} + \frac{z}{x}\vec{K}_T, \tag{6}$$

where p_T, is the transverse momentum of a secondary produced in a chain with respect to the CMS of the chain and $\vec{p}_T$ is the corresponding in the over-all CMS and z and x are respectively the light cone variables of the secondary and of the constituent at the end of the chain. Squaring both sides of Eq. (6) and averaging with respect to $\vec{p}_{T'}$ and $\vec{K}_{T'}$ one obtains

$$\langle p_T^2\rangle = \langle p_{T'}^2\rangle + \left(\frac{z}{x}\right)^2 \langle K_T^2\rangle_k. \tag{7}$$

Here z, x and k (the number of inelastic collisions) are kept fixed. The subscript k is to emphasize that $\langle K_T^2\rangle$ is expected to depend on k. Assuming that the transverse momenta of the virtual particles that "initiate" the chains are statistically independent (except for energy momentum conservation) and normally distributed one obtains

$$\langle K_T^2\rangle_k = \frac{k-1}{k}\langle K_T^2\rangle_\infty. \tag{8}$$

It follows from Eqs. (7) and (8) that there is an increase of $\langle p_T^2\rangle$ with k and therefore with multiplicity (see b). The value of this increase from $k = 1$ to ∞, depends on the unknown quantity $\langle K_T^2\rangle_\infty$ and on the rapidity distribution in the individual chains. For long chains the effect is very small. However, due to the fact that the rescattering chains are short, one can essentially reproduce the observed increase of $\langle p_T\rangle$ with value $\langle K_T^2\rangle_\infty \sim 1$ GeV^2.

If this is the main source of the increase of $\langle p_T \rangle$ with multiplicity, one predicts a well defined rapidity structure of the effect, namely due to the factor $(z/x)^2$ in Eq. (7) one expects the effect to be very small at small values of y. More precisely we obtain a $\delta\langle p_T^2 \rangle$ in the rapidity window $|y| \lesssim 1$ that is one half of the corresponding value in the window $|y| \lesssim 4$. This prediction is very easy to test.

Concerning the energy dependence of the effect, one expects this effect to be much more important at collider than at ISR energies due to the increasing importance of the rescattering chains with increasing s. More precisely, at lower ISR energies the rescattering chains are completely negligible (the long-range forward-backward correlation slope b_{LR} is zero at these energies) and we expect essentially no rise of $\langle p_T \rangle$ with multiplicity. At higher ISR energies (where $b_{LR} \sim 0.15$) the contribution of the rescattering chains begins to be sizeable and one expects a positive correlation which, however, should be smaller than at collider energy.

4. Extension to hadron-nucleus [18] and nucleus-nucleus [19] interactions

The model can be extended in a rather straightforward way to high energy hadron--nucleus and nucleus-nucleus interactions. The fact that multiple inelastic collisions in hadron-hadron interactions involve necessarily different constituents of the colliding hadrons (Fig. 1) reflects a very important property of strong interactions which in turn

TABLE III

The average multiplicities and central densities of negative particles produced in a collision nucleus A–nucleus B at $\sqrt{s} = 31$ GeV per nucleon-nucleon collision. The last two columns are the corresponding values for central (head-on) collisions

A	B	dN^-/dy	$\langle N^- \rangle$	$\left(\frac{dN^-}{dy}\right)^c$	$\langle N^- \rangle^c$
12	27	4.9	22.6	15.5	69.6
12	108	8.2	37.4	24.1	108
12	208	10.3	46.8	29.5	132
27	208	18.3	82.7	64.7	286
64	208	33.4	149	139	598
108	208	45.5	203	207	877

implies that there is no conceptual difference between multiple inelastic scattering in hadron--hadron, hadron-nucleus and nucleus-nucleus collisions (except for intra nuclear cascade).

Some recent results in this domain are the following:

1) Long-range forward-backward correlations in hadron-nucleus collisions have been calculated [20]. The correlation slope b_{LR} is much larger than in p–p collisions at the same energy. A sizeable value of this slope is predicted at 200 GeV/c (in p–p collisions $b_{LR} \sim 0$ up to lower ISR energies).

2) Average multiplicities and central rapidity densities in nucleus-nucleus collisions have been computed [21]. Particular attention has been given to the case of central (head-on) collisions. Some results are given in Table III. It follows from these results that for a head-on

Ag–Pb collisions at $\sqrt{s} = 31$ GeV per nucleon-nucleon collision one expects an energy deposition of about 3 GeV/fermi^3 which seems to be sufficient to produce a phase transition to a quark-gluon plasma.

5. *Conclusions*

The multi-chain dual parton model isbased on very general principles. It is formulated in the framework of an S-matrix theory with unitarity constraints explicitly taken into account. It provides a unified description of multi-hadron production in hadron-hadron, hadron-nucleus and nucleus-nucleus interactions. Once the relative weights of the various multiple scattering terms have been determined from standard unitarization schemes, the model contains no adjustable parameter. The model has a real predictive power. Many features of the collider data were predicted by the model. The existing data are well accounted for at a quantitative level. Moreover, the collider results at low p_T can be understood, at a semi-quantitative level from the basic features of the model. The physical origin of the results is thus very transparent.

REFERENCES

[1] J. C. Rushbrooke, XXI Int. Conf. on High Energy Physics, Paris 1982, ed. P. Petiau and M. Portneuf.
[2] A. Capella, A. Krzywicki, *Phys. Rev.* **18D**, 4120 (1978).
[3] See A. Capella, J. Tran Thanh Van, *Phys. Lett.* **114B**, 450 (1982); *Z. Phys.* **18**, 85 (1983) and references therein.
[4] G. t'Hooft, *Nucl. Phys.* **B72**, 461 (1974).
[5] G. Veneziano, *Nucl. Phys.* **B74**, 365 (1974); **B117**, 519 (1976).
[6] M. S. Dubovikov et al., *Nucl. Phys.* **B123**, 147 (1977); See also A. B. Kaidalov, K. A. Ter-Martirosyan, preprint ITEP-51 (1982).
[7] A. Capella, J. Kaplan, J. Tran Thanh Van, *Nucl. Phys.* **B97**, 497 (1975).
[8] A. Capella, U. Sukhatme, Chung-I Tan, J. Tran Thanh Van, *Phys. Lett.* **81B**, 68 (1979); *Z. Phys.* **3**, 329 (1980); A. Capella, U. Sukhatme, J. Tran Thanh Van, *Phys. Lett.* **125B**, 330 (1983).
[9] S. J. Brodsky, J. Gunion, *Phys. Rev. Lett.* **37**, 402 (1976) and SLAC-PUB-1820.
[10] A. Capella, Proc. of the Europhysics Study Conference, Erice, Italy 1981, ed. R. T. Van de Walle.
[11] UA1 Collab., *Phys. Lett.* **107B**, 320 (1981); UA5 Collab., *Phys. Lett.* **107B**, 310 (1981).
[12] K. Fiałkowski, A. Kotański, *Phys. Lett.* **107B**, 132 (1981).
[13] F. Bopp, Univ. of Siegen preprint (1982); T. Kanki, Osaka Univ. preprint.
[14] UA5 Collaboration, K. Alpgärd et al., *Phys. Lett.* **123B**, 361 (1983).
[15] P. Carlson, Proc. of the XI Int. Winter Meeting, Toledo 1983.
[16] A. Capella, A. Krzywicki, Orsay preprint 83/12.
[17] G. Arnison et al., *Phys. Lett.* **118B**, 167 (1982).
[18] A. Capella, J. Tran Thanh Van, *Phys. Lett.* **93B**, 146 (1980); *Z. Phys.* **C10**, 249 (1981).
[19] A. Capella, J. Kwieciński, J. Tran Thanh Van, *Phys. Lett.* **108B**, 347 (1982).
[20] A. Capella, J. Tran Thanh Van, Orsay preprint 83/10.
[21] A. Capella, C. Pajares, A. Ramallo, in preparation.
[22] A. Capella, J. Tran Thanh Van, *High moments of the $\bar{p}p$ multiplicity distribution in the dual parton model*, to be published in *Z. Phys.*
[23] Ames-Bologna-CERN-Dortmunt-Heidelberg-Warsaw Collab., A. Breakstone et al., CERN preprint (1983).
[24] UA5 Collaboration, CERN-EP/84-04.
[25] W. Thomé et al., *Nucl. Phys.* **B129**, 365 (1977).